Open access • Journal Article • DOI:10.1051/JPHYS:01989005008093700

Electron microscopy observations of the incommensurate phase in berlinite and quartz : interference contrast in the c-zone axis conditions — Source link

Etienne Snoeck, H. Mutka, Christian Roucau

Institutions: Centre national de la recherche scientifique

Published on: 01 Apr 1989 - Journal De Physique (Société Française de Physique)

Electron microscopy observations of the incommensurate phase in berlinite and quartz : interference contrast in the c-zone axis conditions

Etienne Snoeck, H. Mutka, Christian Roucau

J. Phys. France **50** (1989) 937-948 15 AVRIL **1989**, PAGE 937

Classification
Physics Abstracts
61.16D — 61.50E

Electron microscopy observations of the incommensurate phase in berlinite and quartz : interference contrast in the *c*-zone axis conditions

E. Snoeck, H. Mutka (*) and C. Roucau

Laboratoire d'Optique Electronique du CNRS, B.P. 4347, 31055 Toulouse Cedex, France

(*Reçu le 16 novembre 1987, révisé le 16 décembre 1988, accepté le 16 décembre 1988*)

Résumé. — La phase incommensurable triplement modulée de la berlinite et du quartz est imagée par microscopie électronique dans l'orientation correspondant à l'axe de zone *c*. Une étude systématique des images et des taches de diffraction satellites révèle que les contrastes en forme de triangles sombres et clairs obtenus avec le faisceau transmis ou une réflexion *hk*0 et les satellites qui l'entourent, peuvent être expliqués par un modèle de contraste d'interférences analogue à celui des images des plans réticulaires à haute résolution. Cette image d'interférence est en accord avec la relation de phase de la triple modulation incommensurable obtenue par minimisation de l'énergie libre selon les travaux théoriques existants.

Abstract. — The triply modulated incommensurate phase of berlinite and quartz is imaged by electron microscopy in *c*-zone axis orientation conditions. The systematic study of the images and of the incommensurate diffraction satellites shows that the apparently triangular dark/light contrast pattern obtained with the transmitted beam or a general *hk*0-reflection and the surrounding satellites can be explained by an interference contrast model similar to that for usual high resolution lattice imaging. This interference image is consistent with the phase relation of the triple incommensurate modulation conjectured by the minimisation of the free energy, according to the existing theoretical work.

1. Introduction.

The incommensurate phase of quartz (SiO_2) and berlinite ($AlPO_4$) [1] is one of the fascinating features of these materials that are interesting both for basic research and applications. Near the α-β phase transition, which has been known for almost a century in quartz [2], anomalies were recently observed that led to the discovery of the incommensurate phase in both materials [3-5]. Earlier electron microscopy imaging had already revealed between the α- and β- phases an apparently triangular ordered structure at about 10 nm scale [6, 7] which was originally interpreted as a regular arrangement of the low temperature α-

(*) *Present address :* Institut Laue-Langevin, 156-X, F-38042 Grenoble Cedex, France.

phase twins. Later theoretical work conjectured the existence of an incommensurate phase [8]. The studies carried out ever since have revealed the rich variety of phenomena that occur in the incommensurate phase of berlinite and quartz [9-14].

In spite of the pioneering results obtained in transmission electron microscopy the later development has evoked doubts concerning the interpretation of the electron microscope observations. One of the particular objections was that the α-phase microtwin model of the triply incommensurate phase is not in agreement with the diffracted intensities in x-ray experiments [15] even though it seemed to explain reasonably well the contrast in electron microscopy [16]. On this basis it was argued that in the electron microscope one cannot observe the true incommensurate phase but only a transient interface structure. The recent observation of electron diffraction satellites [17, 18], in good agreement with x-ray and neutron diffraction [1, 4, 5, 10], already indicated that the same incommensurate phase can be studied by all these methods. Moreover, it was found out [17] that very regular triangular images can be recorded in the *c*-zone axis conditions, i.e. using the reflections of the *hk*0 reciprocal plane. This observation was in apparent contradiction with earlier electron microscopy work [6, 7] in which the triangular contrast was clearly visible only by using the basic reflections that show a different structure factor for the α-phase twins and that cannot be found in the *hk*0 reciprocal plane. The aim of the present report is to demonstrate that the images observed in the *c*-zone axis conditions do not depend on the structure factor of the basic *hk*0 reflection but can be understood by treating the contribution of the incommensurate satellites correctly. Actually a contrast model based on interference between the satellites and a basic reflection can account for the experimental observations. The observed interference image is in good agreement with the proposed structural models that assume a displacement mode with Σ_2 symmetry. This symmetry describes the atomic displacements of the β-α transition and was proposed in the first theoretical work [8] for the incommensurate modulation. It has been conserved in the more detailed model based on the coupling of the soft mode of the α-β transition to the transverse acoustic (c_{66}) mode [19]. As a consequence, while the α-phase microtwin structure is a possible limit near the lock-in transition, the structural model based on α-phase microtwins is not an absolute necessity for explaining the electron micrographs and its validity cannot be verified by electron microscopic observations.

2. Experimental methods.

The narrow range of stability (about 2 K in quartz, about 4 K in berlinite, at temperatures close to 850 K) of the incommensurate phase in these insulating materials necessitates precautious electron microscope observations. The samples, prepared by ion beam thinning, were covered with a thin layer of amorphous carbon to avoid electrostatic charging and mounted on copper grids with silver paint to ensure good thermal contact. We used simple tilt heating holders coupled with a high precision programmable temperature control in order to facilitate the search of the phase transition and the subsequent imaging. Radiation damage was minimised by observing the samples only in the vicinity of the α-incommensurate-β transition at temperatures around 850 K where the radiolytic defect production rate is slow [20, 21]. Temperature gradients due to non-uniform heating of the thin samples were unavoidable but usually limited below ~ 0.1 K/μm which permitted to obtain reasonably homogeneous images. The heating effects of the electron beam were negligible except with an extremely condensed beam. A JEOL 200 CX microscope with an operating voltage of 200 kV was mainly used for imaging and the high resolution diffraction patterns were obtained at an operating voltage of 120 kV in a Philips EM 400 microscope equipped with a field-emission gun.

3. Triangular contrast at *c*-zone axis orientation.

Figure 1 shows a typical image obtained selecting a 110 reflection and its incommensurate satellites by the contrast diaphragm. Here we want to point out that the selection of only the basic reflection or only one or several satellites is practically impossible because the satellites are so close ($q \sim 10^{-2}$ a*) to the basic reflection. The orientation of the sample is very close to the exact *c*-zone axis : under diffraction conditions, the equivalent *hk*0 basic reflections are equally excited. The contrast is very sensitive to any change of orientation and it can be obtained only by observing the image while adjusting the orientation of the sample very carefully. When deviating from the symmetric excitation conditions the image rapidly degenerates to give patterns where only one or two fringe orientations are clearly seen, as for example in figure 11(a) in [17]. Even in such imaging conditions certain properties (e.g. orientation and period) of the incommensurate modulation can be accurately examined.

The quite regular equilateral triangular pattern is characteristic of a single orientation variant of the incommensurate modulated phase. Images like that of figure 1 and the associated diffraction patterns confirm the triple q character of the modulation. Moreover they have shown us, as concluded earlier [17, 18], that the temperature dependence of the modulation wave vector observed in the electron microscope is in good agreement with the results obtained by x-ray or neutron diffraction in more homogeneous temperature conditions.

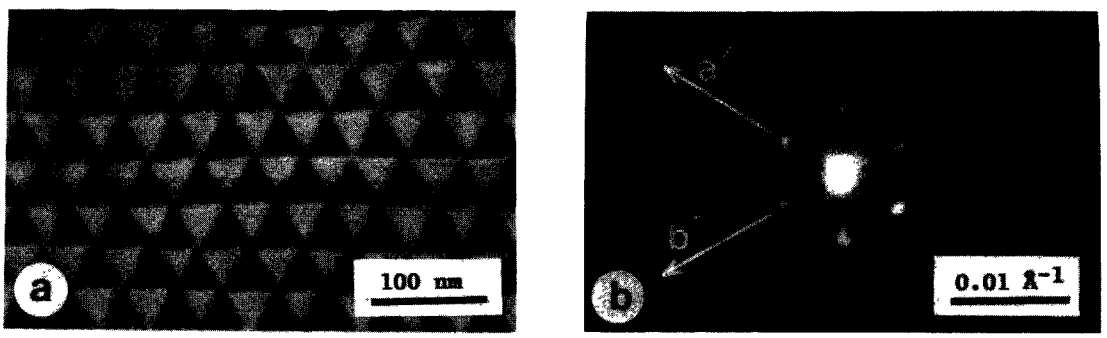

Fig. 1. — (a) Dark field image of the incommensurate phase of quartz obtained with a 110 basic reflection and its satellites ; (b) the corresponding diffraction pattern obtained in equivalent (but not exactly the same) conditions shows the incommensurate satellites around the basic 110 spot.

Triangular contrasts in electron micrographs were observed in the earlier studies [6, 7] but most observations were done in orientation conditions different from those we have currently used. The best contrasts were reported for dark field images with the 301 basic reflection that gives a structure factor contrast for the α-phase twins but that lies outside the *c*-zone axis. Some observations using the *c*-zone axis reflections were reported and the weak contrast was then explained as a result of the violation of Friedel's law in dynamic conditions [7, 16]. In that case no contrast is expected with the direct beam (bright field) [7]. Our results are definitely not in agreement with either of these mechanisms : we have observed the most regular triangular patterns using the direct beam or a general *hk*0 reflection with their respective incommensurate satellites equally excited under the *c*-zone axis conditions. This apparent controversy as well as the existence of well defined diffraction satellites (that were not observed earlier !) led us to search for a new mechanism of contrast formation.

An important clue in our search is the difference between the images obtained with a general *hk*0 reflection and its satellites or with a *h*00 reflection and its satellites. Around the

latter the first order satellites $h00(\pm 1)0$ (the reciprocal lattice and the five dimensional indexing are explained in the appendix), lying close to the [100]* direction are weak and thus there is a set of four relatively intense satellites. A systematic extinction of the $h00(\pm 1)0$ satellites was concluded in the first neutron diffraction experiments [1] but more recent x-ray results have shown that this extinction does not occur in the triply incommensurate phase even in the vicinity of the upper stability limit. In our experimental conditions the $h00(\pm 1)0$ satellites are so weak that the image obtained with this group of reflections is distinctively different from the triangular arrangement and, instead, consists of rows of black and white dots as can be seen in figure 2. This observation points out that the contrast depends on the satellites which surround the basic reflection and which unavoidably contribute to the image. A natural explanation is then an interference between the basic reflection and its satellites. Such an interference should produce intersecting sinusoidal fringe patterns whose orientation and spacing are determined by the satellite positions. This kind of image formation is the usual mode for obtaining so-called high resolution lattice images [22].

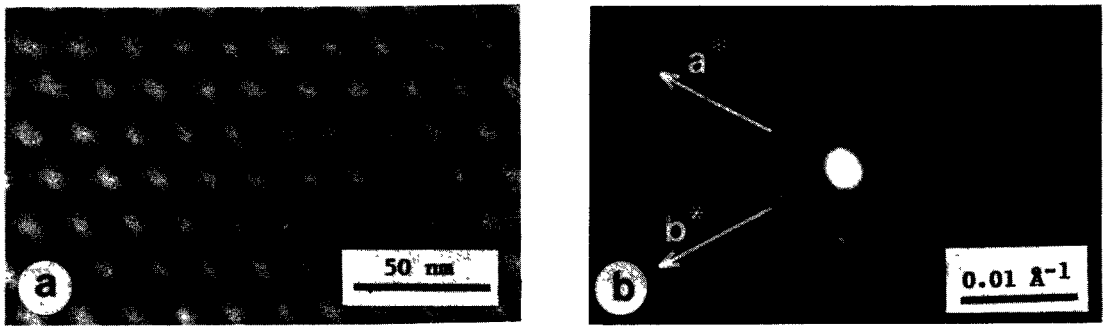

Fig. 2. — (a) Dark field image of the incommensurate phase of berlinite, obtained with a 300 reflection and its four strong satellites that can be seen on (b).

In fact a detailed study of the micrographs, using microdensitometer recordings and a comparison with calculated models has shown that the contrasts observed in figures 1 and 2 are of the form

$$I(r) = I_0 \, \Sigma_i \sin (\mathbf{k}_i \cdot \mathbf{r}) + \text{constant} \qquad (1)$$

where $\mathbf{k}_1$, $\mathbf{k}_2$ and $\mathbf{k}_3$ are three vectors with equal length at 120° from each other, and where we take $i = 1, 2, 3$ for the images obtained using the 000 and $hk0$ basic reflections and their six satellites and $i = 1, 2$ for the $h00$ one with four strong satellites. The good agreement of the interference contrast model of equation (1) with the experimental results can be seen in figures 3 and 4. Figure 3 shows the microdensitometer recording of the observed regular triangular pattern compared with the calculated intensity variation. Figure 4 represents the calculated images that agree very well with the micrographs of figures 1 and 2.

4. A simple model for the interference contrast.

Since there are six strong satellites around the 000 and $hk0$ reflections, it is natural that the interference produces an image whose intensity consists of a superposition of three sinusoidal fringes, equation (1). However, it is not immediately clear why the six satellites produce an image with a trigonal symmetry, or in other words what is the reason for the particular phase relation between the three sinusoidal fringes in equation (1).

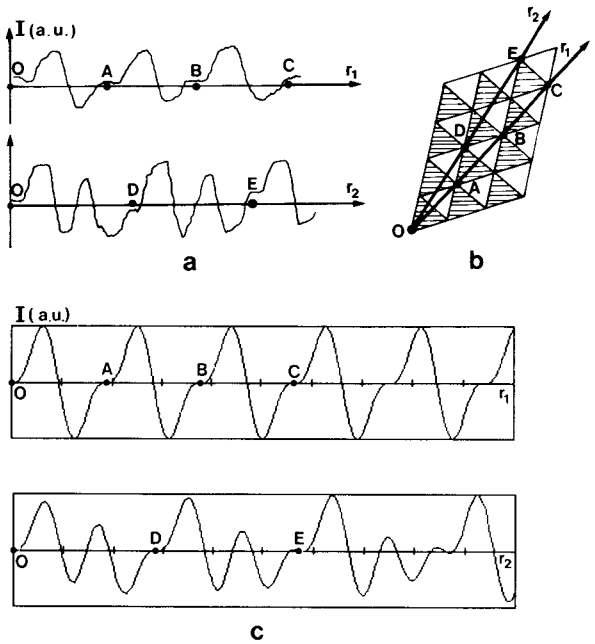

Fig. 3

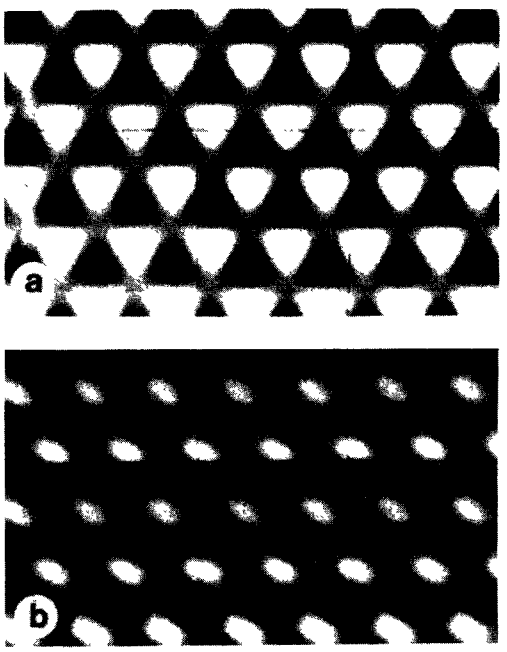

Fig. 4

Fig. 3. — (a) Microdensitometer recording of the image intensity (in arbitrary units, a.u.) along the two directions of the triangular pattern as defined in (b) ; (c) calculated variation of the intensity along the directions in (b) for the sinusoidal fringe model of equation (1). One can see that the general features of the experimental observation on (a) follow quite closely the model.

Fig. 4. — Calculated images corresponding to the model of equation (1). (a) For six satellites ; note that the triangular image is obtained only with the particular phase relation expressed in equation (4) ; (b) for four satellites ; in this case the phases do not affect the form of the image.

To understand why this phase relation is realised, we can examine the image formation in more detail. The general expression for the image intensity for a group of reflections with wavevectors $\mathbf{q}$ and complex amplitudes $a_q \exp(i\phi_q)$ is [22]

$$I(\mathbf{r}) = |\Sigma_q a_q \exp(i\phi\mathbf{q}) \exp(i\, 2\,\pi\mathbf{q}\cdot\mathbf{r})\, T(q)|^2$$
$$T(q) = \exp i\pi\,[(\Delta z\lambda^2 q^2 + C_s\,\lambda^4 q^4/2)/\lambda]\,. \qquad (2)$$

Here $T(q)$ is the transfer function of the electron microscope that depends on the defocus Δz and the spherical aberration coefficient C_s, λ is the electron wavelength. Let us assume a basic reflection with amplitude a_0 and phase ϕ_0 and satellites around it at hexagonal positions $+\mathbf{Q}_i$, $-\mathbf{Q}_i$ ($\mathbf{Q}_i$, $\mathbf{Q}_j$ at 120°), with equal amplitudes $a_Q = a(\pm\mathbf{Q}_i)$ and with phases ϕ_{+i}, ϕ_{-i}. Their interference will produce an image intensity that can be written in the form

$$I(\mathbf{r}) = 4\,a_0\,a_Q \times \Sigma_i \cos\,[(\phi_i + \phi_{-i})/2 - \phi_0] \cos\,[\mathbf{Q}_i\cdot\mathbf{r} + (\phi_i - \phi_{-i})/2] + a_0^2 + 6\,a_Q^2\,. \qquad (3)$$

We have further assumed that the transfer function of the microscope is equal for all the reflections that we have chosen ; this is quite reasonable when considering the smallness of q with respect to the cut-off frequency of the transfer function (in axial conditions

$T(Q) \simeq T(0) = 1$). Now we can see that both the intensity and the relative position of the fringes depend on the phases ϕ_0, ϕ_i of the reflected waves. First we can note that with four satellites the image will not present a triangular texture for any values of ϕ's (see Figs. 2 and 4(b)), and that only its position will depend on the actual phase values. A more interesting situation is that with six satellites. In this case, a triangular image like that in figure 4(a) is obtained only if

$$\phi_i - \phi_{-i} = \pi \mod (2\pi) \quad \text{and} \tag{4a}$$

$$\phi_i = \phi_j \quad \text{for} \quad i \neq j\,. \tag{4b}$$

These phase conditions are necessary to reduce the modulated part of equation (3) to equation (1), that is, to a superposition of three sinusoidal fringes of equal amplitude with a common origin where the three modulation waves have a zero value.

5. Discussion.

5.1 VISIBILITY OF THE INTERFERENCE FRINGES. — We can expect to observe the fringes superposed on the constant background if the amplitude a_Q is large enough with respect to a_0. Neutron diffraction experiments [1, 23] have shown that the satellite intensities ($\propto a_Q^2$) are typically of the order of 10^{-2} times the main Bragg peak intensity ($\propto a_0^2$). With such values ($a_0/a_Q \simeq 10$) the peak-to-peak modulation in equation (3) is about 75 % of the constant background in optimal conditions, i.e. when the phase conditions of equation (4) maximize the modulation and when the ϕ_0 dependent cosine term is equal to ± 1. The observed diffraction patterns and the interference images, for example figure 1, suggest that in the electron microscope the satellite intensity can be comparable to the intensity of the basic reflections. To explain this, we recall that in dynamical conditions the kinematically weak satellite intensities that have large extinction distances can be strongly amplified with respect to the main reflections or to the transmitted beam when the sample thickness corresponds to one of the extinction maxima for the latter [22]. This general remark is particularly helpful to understand the relatively high intensity of the 000mn satellites around the direct beam. In principle their kinematical structure factor is weak in analogy with the $h00(\pm 1)0$ satellites [1, 9, 15].

Another experimental fact is that the satellite intensity (and image quality) changes with extremely small changes of orientation. Qualitatively this is in agreement with the idea that the satellite intensity depends on dynamical diffraction through the main reflections that are not in exact Bragg conditions and whose contribution to the intensity has an exponential dependence on the excitation error [22]. This orientational sensitivity has a twofold consequence on the observation of images. First, subtle changes of orientation can favour the formation of a regular image by compensating for the small differences of the intensities of the satellites that are not expected nor observed [1] to be equal. In this respect we can note that our model calculations using equation (1) have shown that a variation of the order of 25 % of one or two of the sine wave amplitudes (corresponding to roughly 50 % change in satellite intensity) only slightly perturbs the triangular texture of the image. On other occasions the symmetric excitation conditions cannot be achieved and the observed images are deformed, or show only two modulation directions. Such a situation can be reproduced with the model calculations with unequal weights of the sinusoidal fringes.

A characteristic feature of the interference contrast model of equation (3) is that the ϕ_0 dependent cosine term that depends on the sample thickness can attenuate or even suppress the modulated part of the contrast. This is in perfect agreement with the difficulties of the experimentator who sometimes fails in looking for the triangular contrasts in spite of

accurate orientation and temperature control, and who then suddenly succeeds after having found the right point of observation where the sample thickness is close to optimal.

5.2 RELATION WITH THE INCOMMENSURATE STRUCTURE. — For a thin sample one can expect the diffraction patterns and micrographs obtained in the *c*-zone axis conditions to be characteristic of the two dimensional projected potential of the sample crystal in the *a-b* plane and insensitive to any symmetry elements that depend on the structure along the *c*-axis [22]. This is sufficient for the study of the incommensurate modulation that extends only into the *a-b* plane in the sense that there is no modulation along the *c*-axis. The diffraction patterns are clearly of sixfold symmetry. This means that the point group of the projected potential is at least of order three and that it can be of order six. If the projected potential itself has a sixfold symmetry we are in the centrosymmetric situation (for the projected potential). In this case the interference image will be a true image of the projected potential, i.e. the positions of the interference fringes do not depend on the sample thickness, or on the defocus of the microscope [22].

According to x-ray observations the basic reflections have the same intensities in the β- and incommensurate phases [15] which means that the average structure in this case has the $P6_222$ symmetry, and that the projected potential of the average structure has a sixfold symmetry. The symmetry of the triply modulated incommensurate phase will depend on the displacement mode of the modulation. The presentation of resulting symmetry in the superspace formalism [24, 25] is briefly outlined in the appendix in the case of a displacement mode that is invariant in a threefold rotation around the *c*-axis but shows an inversion of the atomic displacements under twofold (and sixfold) rotation. This is in agreement with the Σ_2 symmetry that is expected for the displacement mode of the incommensurate phase [9, 19] (see also [1]). Accordingly, the displacement pattern consists of a single triply modulated mode

$$\mathbf{u}_j(\mathbf{r}) = \mathbf{u}_{j0}\, \Sigma_i \sin\, (\mathbf{Q}_i \cdot \mathbf{r} + \psi_i) \tag{5}$$

with

$$\psi_i = 0 \mod (2\,\pi)$$

(here $\mathbf{u}_j$ refers to the displacement of atom j in the unit cell, and the vectors $\mathbf{Q}_i$ are of equal length and at 120° of each other). The structure modulated by these atomic displacements has a sixfold point group. Consequently, as discussed above, even in dynamical diffraction conditions the observed interference image is a true image of the projected potential of the crystal. Indeed in our experiments it is verified that the relative positions of the interference fringes do not change with the imaging conditions such as defocus or sample thickness. We can thus associate the phase relation of the interference fringes, equation (1) or (4a), with the phase relation of the modulation waves in equation (5).

One may now wonder why a sixfold symmetric potential gives a triangular image, or what are the black and white « triangles » on the micrograph. According to the interference image formation the colour is associated with the phase of the potential, the black region corresponds to a given sense of displacements and the white one to the opposite sense, as depicted in figure 5. In fact there is an ambiguity concerning the absolute colour of a given type of « triangles » that can be black or white depending on the reference phase.

We have shown above that in the *c*-zone condition a microdomain structure is not necessary to explain the regular « triangular » images. On the other hand, even a microdomain structure can be in agreement with our results, as long as the domain variants are related by a change of sign in the atomic displacement pattern. In particular, the α_1/α_2 microdomains fulfill this requirement. Independently of the exact nature of the displacement mode the development of a domain structure with sharp interfaces proceeds by the increase of the higher harmonics

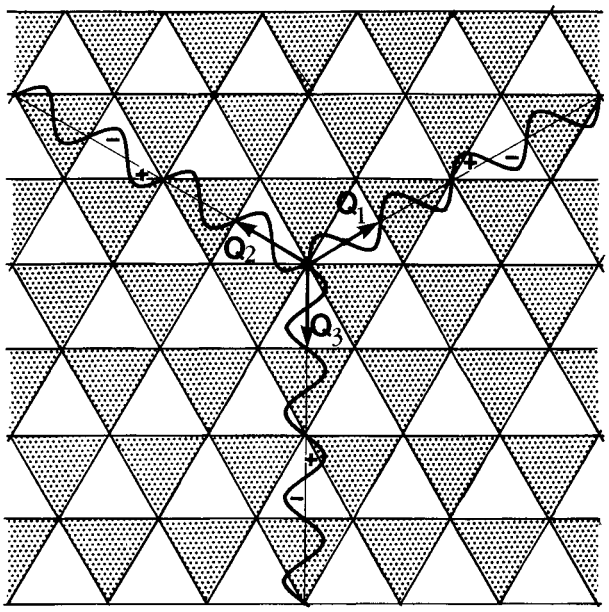

Fig. 5. — A model for the incommensurate modulated structure as a sum of three equal amplitude modulation waves. Dark/light triangles correspond to +/− sign of displacements. A twofold rotation of the pattern turns the triangles to point to the opposite direction but simultaneously changes the colour of the triangles.

content (reflections at $2\,q_i$, $q_i + q_j$ etc.). Even though harmonics can be observed in diffraction mode, it is not meaningful to try to extract in detail their contribution from our results. As can be seen in figures 3 and 4, the observed images can be well explained using the first satellites only and accordingly the role of harmonics seems to be less than the experimental error.

5.3 INTERFERENCE CONTRAST OUTSIDE THE *c*-ZONE AXIS. — As far as our results are concerned the α_1/α_2 type microdomain structure is not necessary for the interpretation of the images. However, under other conditions, the observed contrast has been explained by the structure factor difference and this is the point we want to discuss now. In a recent study [26] the incommensurate satellites were observed by electron diffraction in association with images. Quite remarkably, in the *c*-zone axis observations the geometrical relation of the satellites and of the fringe-like image corresponds exactly to the present interference model even though this possibility was not considered in the paper. In figures 3 and 4 of reference [26] only two dominating fringe orientations are visible in the image obtained with a 100 basic reflection and its four relatively strong satellites. But what is even more interesting is the image obtained using the 301 reflection. Figure 2 in reference [26] is a good example of the distinctive structure factor contrast for the α-phase twins observed near the incommensurate-α phase boundary. However, at higher temperatures, interference fringes clearly due to satellites are observed well inside the incommensurate phase. In figure 3(b) of reference [26] a single incommensurate satellite of the 301 reflection is strongly excited and only one fringe direction is visible, perpendicular to the satellite wavevector, as expected. On another region of the same sample at slightly different orientation conditions, two satellites and two sets of intersecting fringes are observed, see figure 3(c) of reference [26]. These observations show

that the contribution of the contrast due to the interference of the satellites and the main reflection can overcome the structure factor contrast. It seems that there is a kind of crossover from the interference dominated contrast to the structure factor type with decreasing temperature, when the amplitude of the modulation wave increases. The situation is qualitatively similar to that reported in the layer compound 2H-$TaSe_2$ when going from the triply incommensurate phase to the stripe phase [27].

6. Conclusion.

Our interpretation of the electron microscope images of the incommensurate phase of quartz and berlinite obtained in *c*-zone axis conditions was developed after a systematic examination of the diffraction satellites. Accordingly we were conducted to use an interference contrast model that accounts for the experimental observations quite well and is in agreement with the theoretical predictions concerning the symmetry of the incommensurate phase. We have seen that the electron microscopy observation can be interpreted without an *a priori* supposition of the α-phase microtwin structure. In spite of the inhomogeneous conditions we observe the same incommensurate phase as that examined in neutron and x-ray experiments. When the temperature is varied, for example in the presence of a thermal gradient, we can see large spatial variations of the incommensurate period, associated with localised defects that are characteristic of the material [17, 18].

The earlier electron microscopy results of these materials had been criticised mainly because of the too restrictive interpretation of the early observations as an α-phase microtwin structure. We want to point out that the detailed nature of the displacement mode occurring in the incommensurate modulation cannot be determined by electron microscopy. The similar dependence of the structure factor contrast on the operating reflection in the incommensurate and the α-phase is only a qualitative indication of the nature of the local atomic displacements. This is not, however, a reason for discarding the unique possibilities of electron microscopy for the study of intrinsic defects and kinetic phenomena of the incommensurate phase on the spatial scale of the modulation wavelength [17, 18].

Acknowledgments.

We are grateful to Drs. M. Vallade, B. Capelle and P. Saint-Grégoire for useful discussions and to P. Spiesser for the simulated images. We want to thank Prof. A. Janner, one of the referees of this paper, for corrections and comments concerning the superspace formalism. H. Mutka wishes to thank the Academy of Finland for a travel grant that permitted his visit to the Laboratoire d'Optique Electronique.

Appendix.

SUPERSPACE SYMMETRY OF THE INCOMMENSURATE PHASE OF QUARTZ AND BERLINITE [24, 25]. — The diffraction pattern of the incommensurate phase of quartz and berlinite can be indexed by adding two linearly independent reciprocal lattice vectors $\mathbf{q}_1$ and $\mathbf{q}_2$ to the normal hexagonal system $\mathbf{a}^*$, $\mathbf{b}^*$ (see Fig. 6). We can take

$$\begin{aligned} \mathbf{q}_1 &= \alpha\mathbf{a}^* + \beta\mathbf{b}^* \\ \mathbf{q}_2 &= -\beta\mathbf{a}^* + (\alpha + \beta)\mathbf{b}^* . \end{aligned} \tag{A.1}$$

Consequently the Bravais lattice of the incommensurate phase is No. 80, $P6/m(\alpha\beta 0)$ [24]. A two-dimensional internal space is necessary to construct a five dimensional direct product (super)space to describe the structure. The transformation operations $\{R_s|\mathbf{v}_s\}$ of the

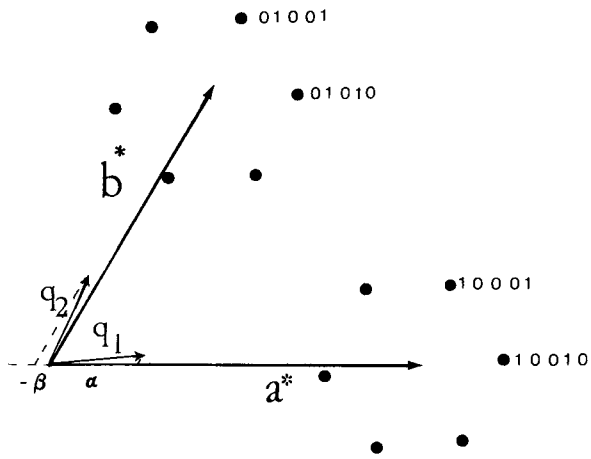

Fig. 6. — The satellites in reciprocal lattice of the modulated phase can be presented with the two linearly independent vectors $\mathbf{q}_1$ and $\mathbf{q}_2$ that span a two-dimensional hexagonal lattice. They can be then indexed in the five dimensional superspace as depicted in the figure. For clarity the lenght of q has been exaggerated, in reality it is only of the order of $10^{-2}\,a^*$.

supercrystal consist of two components, the first one acting in the normal (external) space and the second in the internal space

$$\{R_s|\mathbf{v}_s\} = \{(R_E, R_I)|\mathbf{v}_E, \mathbf{v}_I\} \,. \tag{A.2}$$

The external components of the superspace group generators can be chosen as the operators (2) and (4) among the generators of the space group $P6_222$ (No. 180) [28] of the basic β-quartz structure. The superspace group generators that agree with the Bravais lattice (point group generators) and the symmetry of the basic β-phase are then

$$\begin{aligned} g_{2s} &= \{(3_z^+, 3)|002/3, \mathbf{v}_{I2}\} \\ g_{4s} &= \{(2_z, 2)|000, \mathbf{v}_{I4}\} \,. \end{aligned} \tag{A.3}$$

The generator g_{2s} for the other enantiomorphic variant (space group No. 181) would have the external translation component 1/3c. The internal translation components, $\mathbf{v}_{I2}$ and $\mathbf{v}_{I4}$ depend on the modulation pattern. They can be determined by examining the action of the generators (A.3) on the displacively modulated lattice that is defined by the atom positions (for atom j in the n-th unit cell)

$$\begin{aligned} \mathbf{r}(n, j) &= \mathbf{r}_0(n, j) + \mathbf{u}_j(\mathbf{r}) \\ \mathbf{u}_j(\mathbf{r}) &= \Sigma_{\mathbf{q}}\, \mathbf{f}_j(\mathbf{q}) \exp(i\mathbf{q} \cdot \mathbf{r}(n, j)) \,. \end{aligned} \tag{A.4}$$

As detailed in [25] the symmetry conditions for the modulated lattice are

$$\begin{aligned} R\mathbf{f}_j(\mathbf{q}) &= \mathbf{f}_{j'}(R\mathbf{q}) \exp(iR_s\, \mathbf{q}_s \cdot \mathbf{v}_s) \\ g\mathbf{r}_j &= \mathbf{r}_{j'} + \mathbf{u}(g, j) \end{aligned} \tag{A.5}$$

where $\mathbf{u}(g, j)$ is a translation vector of the basic lattice. Here the operation R_s acts in the superspace, i.e.

$$R_s\, \mathbf{q}_s \cdot \mathbf{v}_s = (R_E\, \mathbf{q} \cdot \mathbf{v}_E, R_I\, \mathbf{q}_I \cdot \mathbf{v}_I) \,. \tag{A.6}$$

For the triple q incommensurate phase of quartz (or berlinite) it has been proposed that the lattice modulation is of the form

$$\mathbf{u}_j(\mathbf{r}) = \mathbf{u}_j \, \Sigma_k \sin \, (\mathbf{Q}_k \cdot \mathbf{r} + \psi_k) \tag{A.7}$$

with $\mathbf{Q}_1 = \mathbf{q}_1$, $\mathbf{Q}_2 = \mathbf{q}_2 - \mathbf{q}_1$, $\mathbf{Q}_3 = -\mathbf{q}_2$ in terms of the reciprocal vectors of equation (A.1). Comparing with the equation (A.5) we can deduce that

$$\begin{aligned} \mathbf{f}_j(\mathbf{Q}_k) &= (1/2)\, \mathbf{u}_j \exp i\,(\psi_k - \pi/2) \\ \mathbf{f}_j(-\mathbf{Q}_k) &= (1/2)\, \mathbf{u}_j \exp -i\,(\psi_k - \pi/2) \end{aligned} \tag{A.8}$$

knowing that $\mathbf{u}_j(\mathbf{r})$ is real. According to theoretical considerations [9, 19] it is expected that the lattice displacement field has the Σ_2 symmetry, i.e. it is invariant in the threefold rotation but changes sign in the twofold rotation. By consequence, if we apply the generator g_{2s}, equation (A.5) gives

$$R_2\, \mathbf{f}_j(\mathbf{Q}_k) = \mathbf{f}_{j'}(R_2\, \mathbf{Q}_k) \exp i R_{2s}\, \mathbf{Q}_{ks} \cdot \mathbf{v}_s \,. \tag{A.9}$$

For example taking $k = 1$, and knowing that $R_2\, \mathbf{u}_j = \mathbf{u}_{j'}$, $R_2\, \mathbf{Q}_1 = \mathbf{Q}_2$, and $R_{2s}\, \mathbf{Q}_{1s} \cdot \mathbf{v}_{s2} = 2\,\pi\,(v_{I2,1} - v_{I2,2})$, we get

$$\mathbf{u}_j \exp i\,(\psi_1 - \pi/2) = \mathbf{u}_j \exp i\,[\psi_2 - \pi/2 + 2\,\pi\,(v_{I2,1} - v_{I2,2})] \,.$$

Putting the phase factors equal gives

$$\psi_1 - \psi_2 = 2\,\pi\,(v_{I2,1} - v_{I2,2}) \,.$$

Similarly we get for $k = 2$ and $k = 3$

$$\begin{aligned} \psi_2 - \psi_3 &= -2\,\pi v_{I2,2} \\ \psi_3 - \psi_1 &= 2\,\pi v_{I2,1} \end{aligned} \tag{A.10}$$

We can choose $\psi_1 = \psi_2 = \psi_3 = \psi$ to get $v_{I2,1} = v_{I2,2} = 0$. Next we apply the generator g_{4s} for which we know that $R_4\, \mathbf{Q}_k = -\mathbf{Q}_k$ and $R_4\, \mathbf{u}_j = -\mathbf{u}_{j'} = -\mathbf{u}_j$. This gives us

$$2\,\psi = -\mathbf{Q}_{ks} \cdot \mathbf{v}_s = 2\,\pi v_{I4,1} = 2\,\pi\,(v_{I4,1} - v_{I4,2}) = -2\,\pi v_{I4,2} \tag{A.11}$$

which is only satisfied if $\mathbf{v}_{I4} = 0$ and $\psi = 0$.

Thus equations (A.10) and (A.11) show that the superspace group generators have no internal translation components. In fact the generator

$$g_{6s} = \{(6_z^+, 6), (001/3, 000)\}$$

is alone sufficient for the superspace group that comes to be

$$\mathrm{P6_2}(\alpha\beta 0) \,.$$

The sixfold symmetry of the modulated phase has been concluded earlier [1] and the superspace symmetry was discussed briefly in a recent report [29].

References

[1] For a review see DOLINO G., Incommensurate Phases in dielectrics, Eds. R. Blinc and A. P. Levanyuk (North Holland, Amsterdam) 1986.
[2] LE CHATELIER H., *C.R. Acad. Sci.* (Paris) **108** (1889) 1046.
[3] BACHHEIMER J. P., *J. Phys. Lett.* **41** (1980) L559.
[4] DOLINO G., BACHHEIMER J. P., ZEYEN C. M. E., *Solid State Commun.* **45** (1983) 295.
[5] BACHHEIMER J. P., BERGE B., DOLINO G., SAINT-GRÉGOIRE P., ZEYEN C. M. E., *Solid State Commun.* **51** (1984) 55.
[6] VAN TENDELOO G., VAN LANDUYT J., AMELINKCX S., *Phys. status solidi* (a) **30** (1975) K 11.
[7] VAN TENDELOO G., VAN LANDUYT J., AMELINKCX S., *Phys. status solidi* (a) **33** (1976) 723.
[8] ASLANYAN T. A., LEVANYUK A. P., *Solid State Commun.* **31** (1975) 547.
[9] ASLANYAN T. A., LEVANYUK A. P., VALLADE M., LAJZEROWICZ J., *J. Phys. C : Solid State Phys.* **16** (1983) 6505.
[10] GOUHARA K., KATO N., *J. Phys. Soc. Jpn.* **53** (1985) 1869, *idem* (1985) 1883.
[11] SAINT-GRÉGOIRE P., SCHÄFER F. J., KLEEMANN N., DURAND J., GOIFFON A., *J. Phys. C : Solid State Phys.* **17** 1375 (1984).
[12] ZARKA A., CAPELLE B., DUMAS J. C., *C.R. Acad. Sci.* (Paris) **302** (1986) 523.
[13] DOLINO G., BASTIE P., BERGE B., VALLADE M., BETHKE J., REGNAULT L. P., ZEYEN C. M. E., *Europhys. Lett.* **3** (1987) 601.
[14] BASTIE P., MOGEON F., ZEYEN C. M. E., *Phys. Rev. B* **38** (1988) 786.
[15] KATO N., GOUHARA K., *Phys. Rev. B* **34** (1986) 2001.
[16] VAN LANDUYT J., VAN TENDELOO G., AMELINKCX S., *Phys. Rev. B* **34** (1986) 2004.
[17] SNOECK E., Thesis, Université Paul Sabatier de Toulouse (1986).
[18] SNOECK E., ROUCAU C., SAINT-GRÉGOIRE P., *J. Phys. France* **47** (1986) 2041.
[19] BERGE B., BACHHEIMER J. P., DOLINO G., VALLADE M., ZEYEN C. M. E., *Ferroelectrics* **66** (1986) 73.
[20] HOBBS L. W., PASCUCCI M. R., *J. Phys. France* **41** (1980) C6-237.
[21] PASCUCCI M. R., HUTCHISON J. L., HOBBS L. W., *Rad. Effects* **74** (1983) 219.
[22] SPENCE J. C. H., Experimental High-Resolution Electron Microscopy (Oxford Univ. Press, New York) 1980.
[23] DOLINO G., BACHHEIMER J. P., BERGE B., ZEYEN C. M. E., *J. de Phys. France* **45** (1984) 361.
[24] JANNER A., JANSSEN T., *Phys. Rev. B* **15** (1977) 643.
[25] JANNER A., JANSSEN T., *Acta Cryst. A* **36** (1980) 399.
[26] YAMAMOTO N., TSUDA K., YAGI K., *J. Phys. Soc. Jpn.* **57** (1988) 1352.
[27] KOYAMA Y., ZHANG Z. P., SATO H., *Phys. Rev. B* **36** (1987) 3701.
[28] Int. Tables For Crystallography, vol. A, Ed. T. Hahn (D. Reidel Publ. Co.) 1987.
[29] WALKER M. B., Incommensurate Crystals, Liquid Crystals and Quasi-Crystals, Eds. Scott J. F., Clark N. A., Plenum Publ. Corp. (1987).